Anti-corrosion and wear properties of plasma electrolytic oxidation coating formed on high Si content Al alloy by sectionalized oxidation mode

Libin Dai, Wenfang Li[1], Guoge Zhang, Nianqing Fu, and Qi Duan

School of Materials Science and Engineering, South China University of Technology, Guangzhou 510641, China

E-mail: mewfli@163.com

Abstract. In this study, a uniform and less defective ceramic coating was prepared on high Si content aluminium alloys by a sectionalized plasma electrolytic oxidation (PEO) mode. The PEO process of Al-9 wt. % Si binary alloy was performed under constant current mode followed by constant voltage mode. The surface micrographs and chemical compositions of different samples were analysed by scanning electron microscopy (SEM) and X-ray diffraction (XRD), respectively. Micro-hardness and reciprocal-sliding testers were used to measure the coatings hardness and tribological performance. It was found that the sectionalized PEO mode could produce hard and anti-friction passive oxide layers with smaller holes and fewer cracks on the Al-Si alloy, comparing with the single constant current mode. In addition, the results of polarization curves and electrochemical impedance spectroscopy (EIS) tests conducted in 3.5 wt. % NaCl solution revealed that the coatings obtained by sectionalized PEO mode had a higher corrosion resistance and provided better corrosion protection for Al-Si alloy.

1. Introduction

The increase of silicon content in Al-Si alloy can effectively improve the wear resistance, flowability, and crack resistance meanwhile reduce its thermal expansion coefficient and specific gravity. Therefore, the Al-Si alloy with high silicon content has been widely used in the meter housing, cylinder and piston parts manufacture [1]. However, many Al-Si alloy products need surface treatment before industrial applications due to the inferior hardness and anti-corrosion property of the bare aluminium alloy [2]. Chemical conversion and anodic oxidation are conventional surface treatment techniques used for Al alloys. However, both of them are not appropriate for the high-silicon content aluminium alloy because the Si element is more difficult to be oxidized than Al in the substrate. It will hinder the formation of continuous and uniform films, further resulting in a decline of the whole film layer performance [3, 4].

Plasma electrolytic oxidation has been considered as one of the most effective and eco-friendly methods to promote anti-corrosion and tribological performance of aluminium and its alloys by forming thick and hard ceramic coatings [5, 6, 7, 8, 9]. Mistry, *et al.* [10] had prepared ceramic coatings on eutectic Al-Si alloy as a cylinder wall surface by PEO technology, which had a greater durability in the longer term than the Ni–SiC coating. Wang, *et al.* [11] also successfully fabricated ceramic coatings on ZAl12Si3Cu2NiMg by PEO and systematically studied the coating mechanism at the initial stages. The formation mechanism of PEO coating is very complicated due to the involvement of electro-, theromo- and plasma-chemical reaction in the electrolyte and metal-

Content from this work may be used under the terms of the Creative Commons Attribution 3.0 licence. Any further distribution of this work must maintain attribution to the author(s) and the title of the work, journal citation and DOI.
Published under licence by IOP Publishing Ltd

electrolyte interface [7, 12-14]. It was found that the coating formation of PEO was influenced by current density, additives, the size of silicon, and the defects of local uneven electrical conductivity [15-18]. However, there are few researches involving the effect of sectionalized oxidation mode (SOM) on anti-corrosion and tribological performance of PEO coatings on high Si content Al alloy. Jaspard-Mécuson and Melhem [19, 20] reported that under constant current mode, with the increase of processing time, the sparks turned to micro-arcs, and then to arcs which was detrimental to the coatings. Wang, *et al.* [21] revealed that under constant voltage mode, when the voltage reached set value and kept constant, the intensity of light emitted by arcs was reduced with the proceeding of PEO. Thus, the processing time of constant current mode and constant voltage mode has a significant effect on the microstructures and properties of the coatings on aluminium alloy. It's likely to acquire a good PEO coating on high Si content Al alloy by using both constant current and constant voltage mode and changing their processing time during PEO process.

In this work, two kinds of different PEO modes, namely, single constant current mode and constant current followed by constant voltage mode, were proposed to treat Al-9 wt. % Si alloy. The single constant current mode was set as the control test. The surface morphologies and compositions of coatings were characterized by SEM and XRD, respectively. The anti-corrosion performance and tribological property of the coating were investigated by electrochemical workstation and friction-abrasion testing machine, respectively.

2. Materials and Methods

The casting Al-9 wt. % Si binary alloy (20 mm × 20 mm × 4 mm) was selected as the substrate in this study. The samples were immersed in the electrolyte. A stainless-steel sheet was used as the counter electrode. The SiC abrasive papers of 240, 400, 600, 800 and 1200 grades were used to polish the samples in sequence. The polished samples were then cleaned with acetone for 5 min in an ultrasonic cleaner. After that the samples were thoroughly washed with distilled water and dried in hot air. The PEO process was conducted using a WHD60 bipolar pulse power with a data acquisition system to record the instantaneous current and voltage. The electrolyte was composed of 10 g/L Na_2SiO_3, 2 g/L NaOH and 4 g/L KF. The temperature was controlled below 40 ℃ during the PEO process using a circulating water cooling unit. The positive and negative current densities of the constant current mode were set as 10 A/dm^2 and 2 A/dm^2, respectively. The positive and negative voltage of the constant voltage modes were 400 V and 50 V, respectively.

The PEO experimental apparatus is shown in Figure 1.

The microstructure and surface morphology of the coating was observed by scanning electron microscopy (SEM, Quanta 200) equipped with energy dispersive X-ray spectroscopy (EDS).

The electrochemical behaviour of the coated sample was investigated by potentiodynamic polarization and electrochemical impedance spectroscopy with CHI660D electrochemical workstation in 3.5 wt. % NaCl solution.

The phase composition of the coating was analysed by Philips X'pert MPD X-ray diffraction in grazing incidence of 2°.

The micro-hardness of the coating was analysed by a HMV-2T micro-hardness tester at a load of 50 g with the loading duration of 10 s. The average value of five different positions was recorded as the final film micro-hardness.

The tribological properties of the PEO coatings were evaluated on a SFT-2M reciprocal-sliding test instrument. The GCr15 steel ball with a diameter of 4mm was used as the friction antithesis. The dry sliding was performed at a load of 2 N, a sliding speed of 300 r/min, and sliding radius of 5 mm. The wear rates were calculated by the weight loss of the whole coating.

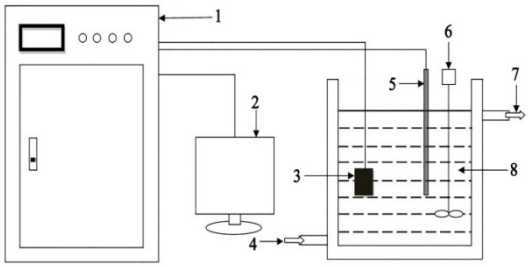

Figure 1. Schematic diagram of the PEO equipment：

1. WHD60 bipolar pulse power, 2. Data processing system, 3. Anode, 4. Circulating water cooling unit, 5. Cathode, 6. Stirring system, 7. Circulating water cooling unit, 8. Electrolyte.

3. Results and Discussion

3.1. The growth process of the coatings in SOM

Figure 2 shows the change of positive voltage over the reaction time in SOM. Table 1 shows the processing time of oxidation modes. In the early stage of the SOM, the voltage rapidly increases and a large number of fine bubbles are produced on the anode surface due to the formation of a passive film on the surface [22]. When the positive voltage reaches to about 160 V, the spark discharges start to appear on the sample surface, and gradually brighten with the increase of voltage. When the voltage is raised to about 240 V, the yellowish arc discharges begin to happen at the corners of the samples because of the high electric field. Around the discharge channel, the deposition of reaction product causes the increase of local resistance and breakdown voltage. Therefore, the sparking area is slowly extended to central part of the samples. At about 280 V, the micro-arcs evenly cover the sample surface.

At the reaction time of 9.5 min, the positive voltage is raised to about 402 V. The 1 # sample is instantly switched into constant voltage mode of 400V and the other samples remain constant current mode. Because the coating resistance is high, the current of 1# rapidly drops to 1 A or less. The average energy of the discharges is decreased, leading to generate uniformly distributed and small sized micro-arcs, as shown in Figure 3.

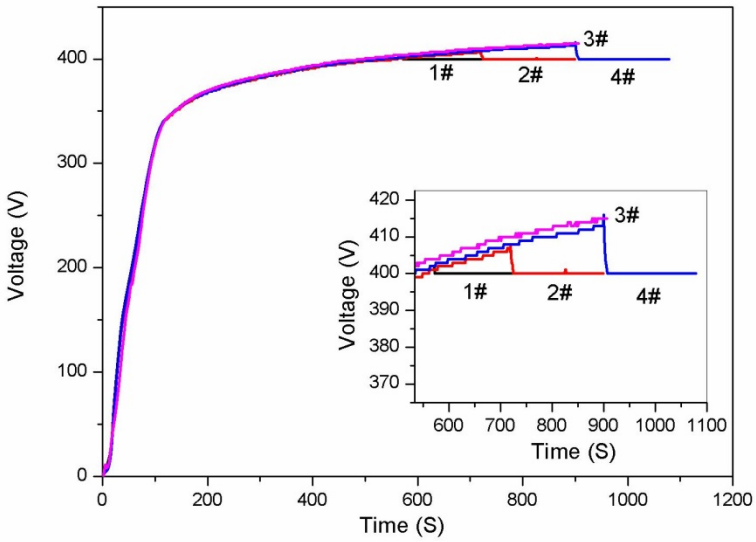

Figure 2. The variation of positive voltage with the PEO processing time for 1#, 2# &4# samples.

Table 1. The oxidation time of constant current mode and constant voltage mode of different samples.

Code of sample	Treatment time of constant current oxidation (min)	Treatment time of constant voltage Oxidation (min)
1#	9.5	5.5
2#	12	3
3#	15	0
4#	15	3

3.2. Microstructure and composition of the oxide film

The surface morphologies of the coatings obtained under different PEO processes are shown in Figure 3. It is obviously seen that the surface of 4# (shown in Figure 3(a) and (b)) is more homogeneous than that of 3# (presented in Figure 3(c) and (d)). In addition, many brightness areas are found on 3# surface. The EDS data reveal that these high brightness areas are mainly composed of silicon oxides (seen in Figure 4). Moreover, there are some cracks can be observed on the 3# surface. By comparison, no cracks are found on the 4# surface. This is attributed to the change in the number of micro-arcs before and after constant voltage oxidation. During constant voltage oxidation, the current density is low and the number of micro-arcs increases. According to the study of Lu [23], the discharges occur preferentially at relatively thin or defective locations. Namely, more micro-arcs appear on the cracked areas. When the molten material is cooled down by the surrounding solution, the residual discharge channels become small and uniformly distributed nodules. It can repair the defects left by the constant current oxidation. Consequently, the sectionalized plasma electrolytic oxidation mode is beneficial to the formation of less defective ceramic coatings on high silicon content Al alloys.

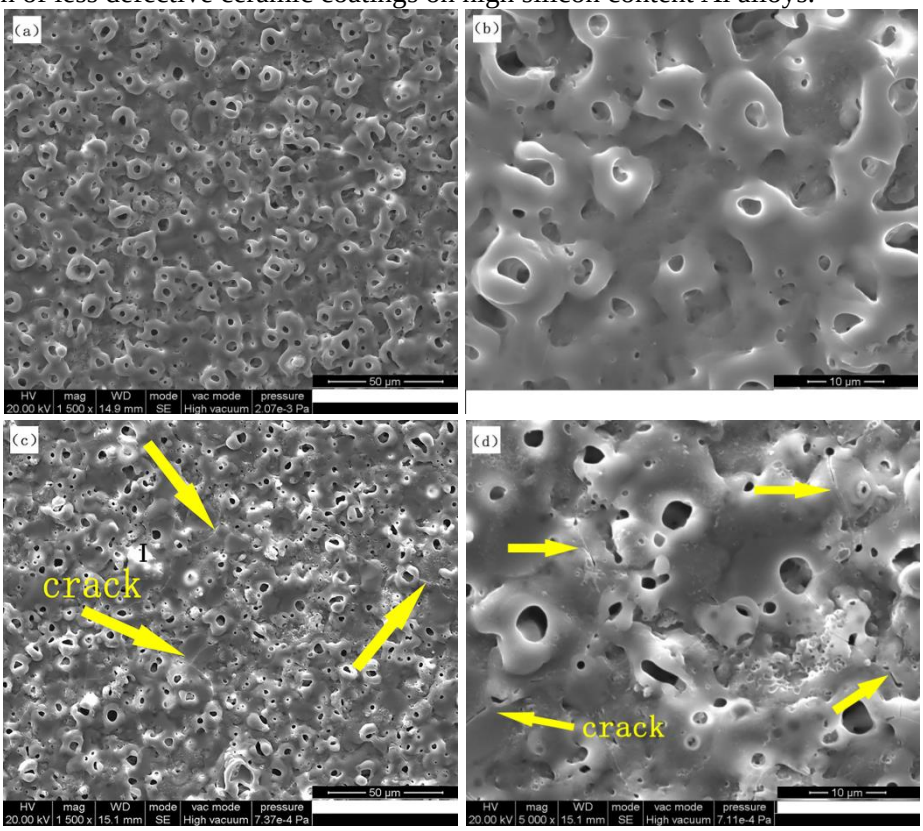

Figure 3. Morphologies of PEO coatings at different oxidation modes: (a, b) constant current oxidation for 15min followed by constant voltage oxidation of 3min. (c, d) constant current oxidation for 15min.

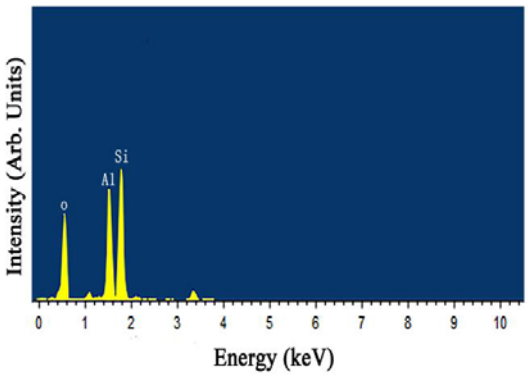

Figure 4. The corresponding EDS spectra of the area marked by I in Figure 3c.

Figure 5 shows the XRD patterns of oxide coatings made by the two different kinds of oxide modes. It can be seen that the plasma electrolytic oxidation coatings are composed of γ-Al_2O_3 and SiO_2. No α-Al_2O_3 or mullite phase is found. Thus, the introduction of sectionalized oxidation mode has little effect on the composition of PEO coating. Researchers [24] found that the content of α-Al_2O_3 and mullite in the PEO coating was increased with the extension of reaction time. The γ-Al_2O_3 does not spontaneously transform to α-Al_2O_3, since the transformation of γ-Al_2O_3 to α-Al_2O_3 needs tremendous energy provided by plasma electrolytic discharge to overcome the energy barrier. Considering that only a short time of 15min is used for the whole PEO process, the energy is not enough to complete this transformation.

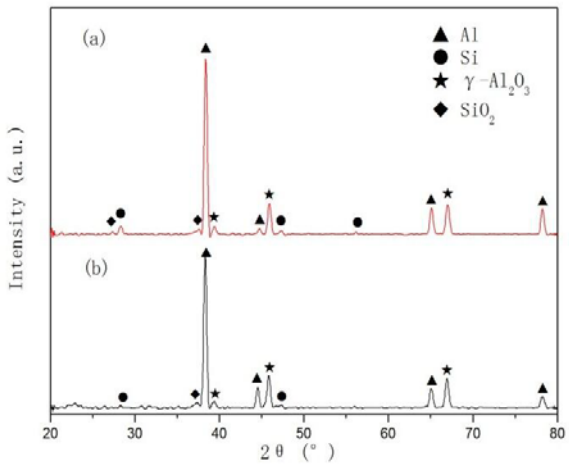

Figure 5. XRD results of the coatings: (a) treated by sectionalized oxidation mode (constant current oxidation for 12min followed by constant voltage oxidation of 3min), (b) treated by single constant current mode.

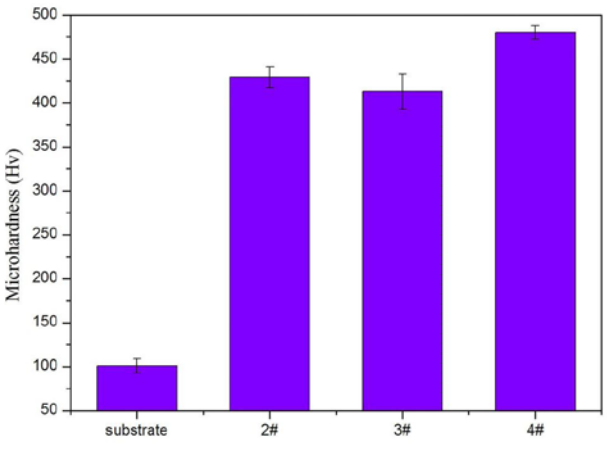

Figure 6. Micro-hardness of PEO coating of 2#, 3#, 4# samples and Al-Si alloy substrate.

3.3. The mechanical and tribological properties of bare aluminium and coatings

The micro-hardness of the films obtained by different treatment processes is shown in Figure 6. The films hardness of 2#, 3#, and 4# is 430Hv, 410Hv, 480Hv, respectively and the hardness of Al- Si substrate is 104Hv. It can be clearly seen that, after PEO treatment, the films micro-hardness is improved over four times higher than that of the Al-Si alloy substrate. This is due to the formation of hard alumina ceramic layer. Comparing 2# with 4#, it is found that longer constant current time producing PEO film with higher micro-hardness when the oxidation time of constant voltage step is

constant. It is because the thickness of dense layer increases with longer galvanostatic polarization time [25]. Meanwhile, when the oxidation time of constant current is constant, the increase of the constant voltage oxidation time improves film's micro-hardness by comparing 3# with 4#. This is considered to be caused by the formation of a more compact passive coating on the specimen surface after longer constant voltage oxidation time treatment.

Figure 7 represents the variation of friction coefficients versus sliding time for the substrate and PEO coatings against Gr15 steal ball under dry friction condition. It is very obvious that there is a great difference on friction properties between the uncoated and coated substrates. The Al-Si alloy substrate records an average friction coefficient of 0.41, while other ceramic coatings under the same test conditions record much larger average friction coefficient around 0.58-0.73. Moreover, no large fluctuations are observed during the wear test. It indicates that there is no coating failure.

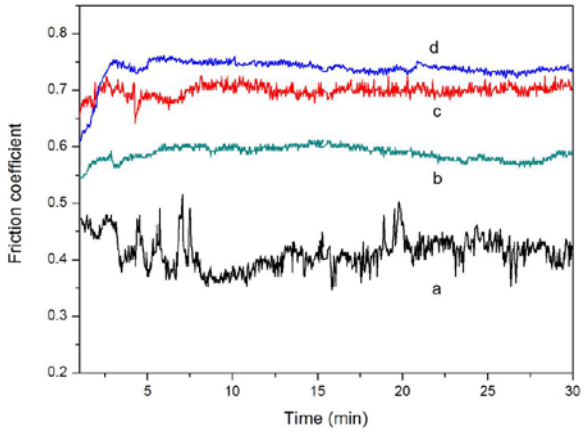

Figure 7. Friction coefficients of bare aluminium and PEO coatings formed at different oxidation modes:

(a) Al-Si alloy, (b) treated by constant current oxidation for 15min followed by constant voltage oxidation of 3min, (c) treated by constant current oxidation for 12min followed by constant voltage oxidation of 3min, (d) treated by single constant current mode.

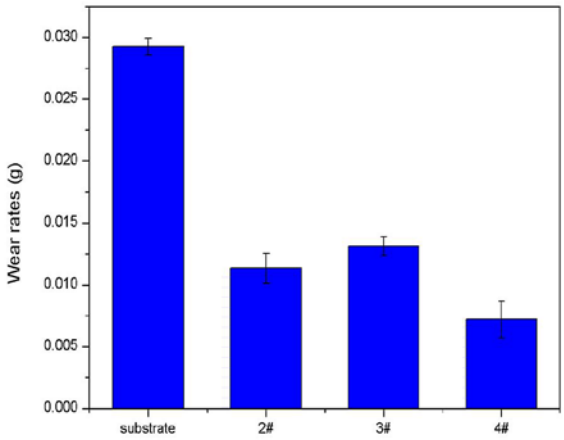

Figure 8. Wear rates of Al alloy substrate and PEO coatings.

The wear rates of bare substrate and PEO coatings are shown in Figure 8. The wear rate of the Al-Si substrate is 29.4 mg, while the wear rates of the coatings are significantly reduced, reaching 7.0-13.2 mg. This clearly indicates that PEO is an effective technology to improve the wear resistance of substrates. Furthermore, the coating treated by constant voltage reveals a smaller wear rate than that of untreated one. This is attributed to the higher micro-hardness (shown in Figure 6) and better compactness (seen in Figure 3) of the coating obtained under constant voltage mode.

3.4. Anti-corrosion study of PEO coatings

In order to study the effect of two different oxidation modes on the corrosion resistance performance of PEO coatings, electrochemical test was carried out. The polarization curves are shown in Figure 9. The corresponding self-corrosion potential and corrosion current density are summarized in Table 2. As seen from Figure 9, after PEO treatment, polarization curves move to a lower current density side. The self-corrosion current density of the PEO processing Al-Si alloy is 10-30 times smaller than that of the pristine substrate and the E_{corr} is improved over 80 mV. It shows that the anti-corrosion performance of the coatings is significantly improved after PEO treatment. In addition,

the self-corrosion current densities of the coatings prepared by the single constant current oxidation mode are higher than those of the sectionalized oxidized coatings. Such results conform to the loose morphologies of the coatings obtained under single constant current oxidation mode. Without constant voltage oxidation, the coatings have more cracks on the surface. These cracks result in the degradation of anti-corrosion performance. In contrast, as mentioned before, the constant voltage oxidation can repair some defects of the coatings produced in the constant current oxidation stage. Therefore, the coating shows an enhanced blocking ability against the etching solution.

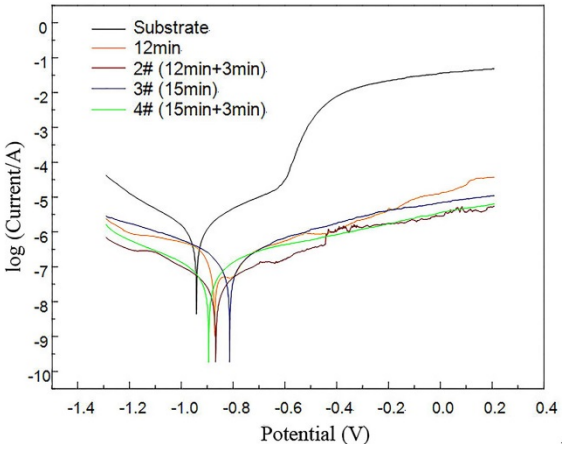

Figure 9. Polarization curves of the substrate and PEO coatings.

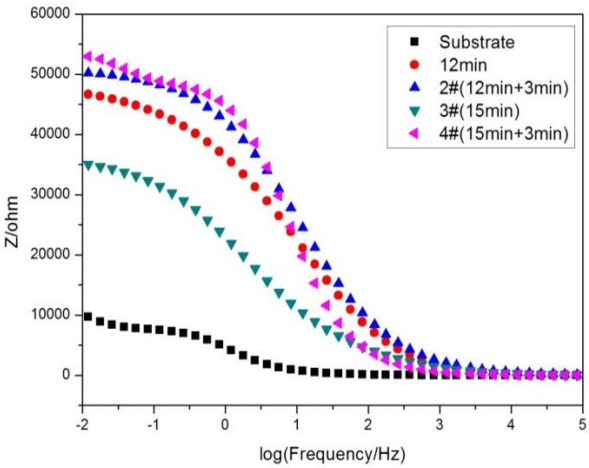

Figure 10. EIS diagrams (Bode) of Al-Si alloy and PEO coatings treated at different processing parameters.

Table 2. Potentiodynamic polarization parameters of different samples: self-corrosion current density (I_{corr}), and self-corrosion potential (E_{corr}).

Sample treatment	I_{corr} ($\mu A/cm^2$)	E_{corr} (V)
C-9% (Substrate)	1.1140	-0.9390
constant current oxidation for 12min	0.1082	-0.8398
2#	0.0335	-0.8216
3#	0.1134	-0.8309
4#	0.0572	-0.8514

The EIS behaviour of bare aluminium and coated samples was investigated after 3600s of immersion. The Bode plots are presented in Figure 10. According to V. Raj, *et al.* [26], the PEO coatings were consisted of outer porous layer and inner compact layer. The anti-corrosion performance of the coating is mainly attributed to the inner barrier layer. In the EIS, the high frequency portion of impedance curves reflects the outer layer properties and the low frequency portion represents the inner layer properties. Thus, the overall polarization resistance values of the substrate and coatings can be evaluated by the extrapolation of the impedance modulus at low frequency [27]. From Figure 10 it can be seen that the resistance of samples is greatly improved after treated by PEO, reaching three to five orders of magnitude higher than that of untreated substrates. Moreover, the introduction of constant voltage oxidation mode after constant current oxidation leads to an improvement of corrosion

resistance performance of coatings, which is in good agreement with the test results of potentiodynamic polarization (in Figure 9 and Table 2).

4. Conclusions

In summary, a sectionalized PEO mode (constant current oxidation followed by constant voltage oxidation) for the treatment of Al-9 wt. % Si alloy had been successfully developed. It was found that the introduction of constant voltage oxidation could repair some defects of the coatings produced in the constant current oxidation stage. Coatings prepared by the SOM technique exhibited a fewer defects, higher micro-hardness (up to 440 Hv) and better anti-wear properties. These resulted in a significant improvement in anti-corrosion performance. The self-corrosion current density of the substrate treated under optimized condition was reduced by around 30 times (from 0.1134 $\mu A/cm^2$ to 0.0335 $\mu A/cm^2$) in comparison with the bare alloy. Moreover, the self-corrosion current density of the coating prepared under SOM mode was lower than that of the coating treated by the conventional single constant current oxidation.

References

[1] Osório W R, Goulart P R, and Garcia A 2008 *Mater. Lett.* **62** 365.
[2] Wang P, Li J, Guo Y, Wang J, Yang Z, and Liang M 2016 J. *Alloys Compd*. **657** 703.
[3] Xu F, Xia Y, and Li G 2009 Appl. *Surf. Sci.* **255** 9531.
[4] Forn A, Picas J A, Baile M T, Martin E, and García V G 2007 *Surf. Coat. Technol.* **202** 1139.
[5] Xiang N, Song R G, Zhuang J J, Song R X, and Su X P 2016 T. *Nonferr Metal Soc.* **26** 806.
[6] Yerokhin A L, Nie X, Leyland A, Matthews A, and Dowey S J 1999 *Surf. Coat. Technol.***122** 73.
[7] Hussein R O, Northwood D O, and Nie X, 2013 *Surf. Coat. Technol.* **237** 357.
[8] Zhu M H, Cai Z B, Lin X Z, Ren P D, Tan J, and Zhou Z R 2007 *Wear* **263** 472.
[9] Hu C J, and Hsieh M H 2014 *Surf. Coat. Technol.* **258** 275.
[10] Mistry K, Priest M, and Shrestha S 2010 Proceedings of the Institution of Mechanical Engineers, Part J: *Journal of Engineering Tribology* **224** 221.
[11] Wang P, Li J P, Guo Y C, Yang Z, and Wang J L 2016 *Surf. Eng*. **32** 428.
[12] Lu X, Blawert C, Huang Y, Ovri H, and Kainer K U 2016 *Electrochim. Acta* **187** 20.
[13] Klapkiv M D 1999 *Mater. Sci.* **35** 279.
[14] Yerokhin A L, Shatrov A, Samsonov V, Shashkov P, Pilkington A, Leyland A, and Matthews A, 2005 *Surf. Coat. Technol.* **199** 150.
[15] Krishtal M M 2004 *Met. Sci. Heat Treat.* **46** 377.
[16] Pan Y K, Chen C Z, Wang D G, Yu X, and Lin Z Q 2012 *Ceram. Int.* **38** 5527.
[17] Mi T, Jiang B, Liu Z, and Fan L 2014 *Electrochim. Acta* **123** 369.
[18] Kazanski B, Kossenko A, Zinigrad M, and Lugovskoy A 2013 *Appl. Surf. Sci.* **287** 461.
[19] Jaspard-Mecuson F, Czerwiec T, Henrion G, Belmonte T, Dujardin L, Viola A, and Beauvir J, 2007 *Surf. Coat. Technol.* **201** 8677.
[20] Melhem A, Henrion G, Czerwiec T, Briançon J L, Duchanoy T, Brochard F, and Belmonte T 2011 *Surf. Coat. Technol.* **205** S133.
[21] Wang L, Chen L, Yan Z, and Fu W 2010 *Surf. Coat. Technol.* **205** 1651.
[22] Hussein R O, and Northwood D O 2014 *Developments in Corrosion Protection* **201**.
[23] Lu X, Blawert C, Kainer K U, and Zheludkevich M L 2016 *Electrochim. Acta* **196** 680.
[24] Wu Z, Xia Y, Li G, and Xu F 2007 *Appl. Surf. Sci.* **253** 8398.
[25] Xue W, Shi X, Hua M, and Li Y 2007 *Appl. Surf. Sci.* **253** 6118.
[26] Raj V, and Ali M M 2009 *J. Mater. Process. Technol.* **209** 5341.
[27] Veys-Renaux, and Rocca E 2015 *J. Solid State Electrochem.* **19** 3121.